Radiative neutrino model with semiannihilating dark matter

Haiying Cai[*]

Asia Pacific Center for Theoretical Physics, Pohang, Gyeongbuk 790-784, Republic of Korea

We propose a two-loop induced radiative neutrino model with hidden gauged $U(1)$ symmetry, in which dark matter of Dirac fermions arises. The relic density gets a contribution from annihilation and semiannihilation due to a residual $\mathbb{Z}_3$ parity. After imposing the requirement of neutrino oscillation data and lepton flavor violation bounds, we find that semiannihilation plays a crucial role in order to satisfy the relic density constraint $0.117 < \Omega h^2 < 0.123$, by proceeding near either one of two deconstructive scalar resonances. Our numerical analysis demonstrates the allowed region for the DM-scalar coupling with the DM mass in (80, 400) GeV.

I. INTRODUCTION

Radiative seesaw neutrino models are one of the attractive scenarios to connect the neutrino sector with the dark matter (DM) sector in a natural manner. These two sectors certainly involve mysterious puzzles that are frequently interpreted as physics beyond the Standard Model (SM). When the neutrino masses are radiatively induced, the magnitude of relevant couplings could reach $\mathcal{O}(1)$ compared with the case where the neutrino mass is generated at the tree level, so the mass hierarchy among the SM sector and heavy fermion or scalar sectors is largely alleviated. Furthermore, new particles that are accommodated in the theory are at the $\mathcal{O}(\text{TeV})$ energy scale and accessible by the extensive search at the Large Hadron Collider (LHC). For the radiative seesaw mechanism, a discrete symmetry is essentially implemented in order to forbid the neutrino mass at the tree level, and such symmetry will in turn stabilize the lightest neutral particle as a DM candidate. As a consequence, this type of theory provides interesting phenomenologies, with the requirement to satisfy the observed relic density of $\Omega h^2 \approx 0.120 \pm 0.001$ [1] and other experimental constraints.

The simplest discrete symmetry can be $\mathbb{Z}_2$, as the remnant of a broken $U(1)$ symmetry, and a typical DM-generated neutrino mass model at the one-loop level is proposed in [2]. However, other enlarged discrete symmetries are also possible to stabilize the DM candidate, such as $\mathbb{Z}_N$, $N > 2$ discrete parity, which

brings in semiannihilation in addition to annihilation for the Lee-Weinberg scenario [3], allowing for an odd number of DM particles appearing in a $2 \to 2$ process [4–7]. Under the control of $\mathbb{Z}_N$ discrete symmetry, any field transforming as $f_i \to \omega^a f_i$, with $\omega = \exp(i2\pi/N)$ and $a = 1, \ldots, N - 1$, could serve as the dark matter candidate depending on the spectrum and interactions. In this paper we consider a two-loop induced neutrino mass model [8–13] with new particles charged under a hidden $U(1)$ symmetry [14–20], in which a Dirac fermion type of $\mathbb{Z}_3$ DM candidate arises, whose relic density is dominantly explained by the s-channel of semiannihilation modes. Note that in this model, it is also possible for a complex scalar to behave as DM in the inverse mass pattern. The discrete $\mathbb{Z}_3$ symmetry originates from the spontaneous breaking of $U(1)$ symmetry and plays an important role to ensure the DM χ does not decay while the reaction in the form of $\chi\chi \to \chi^\dagger v_i$ exits. We present how the DM and neutrino mass are correlated by formulating each sector. In particular, we perform an analysis to obtain the allowed region which satisfies a set of necessary bounds, including neutrino oscillation data, lepton flavor violations (LFVs), muon anomalous magnetic moments (Δa_μ, a.k.a. muon $g - 2$), and the DM relic density.

This paper is organized as follows. In Sec. II, we show the valid Lagrangian with charge assignments and formulate the scalar and neutrino sectors, along with the LFVs, muon $g - 2$, $Z - Z'$ mixing, and the bound of the electroweak precision test. In Sec. III, we analyze the Dirac fermionic DM to explain the relic density with an emphasis on the semiannihilation and a brief illustration of the analytic derivation. In Sec. IV, we conduct a numerical analysis and show the allowed region to satisfy all the phenomenologies that we discuss above. Finally, we give our conclusions and a discussion in Sec. IV.

[*]haiying.cai@apctp.org

II. THE MODEL

The model is built by extending the SM with additional scalars and vectorlike fermions, which are charged under a hidden $U(1)$ symmetry before some of the scalars obtain vacuum expectation values (VEVs). The field contents and their charge assignments are reported in Table I. For the fermion sector, an isospin doublet $L' \equiv [E', N']_i^T$ plus two isospin singlets χ_i and N_i, with $i = 1, 2, 3$, are added. The vectorlike nature of these extra fermions ensures that our extension is anomaly-free. The quantum number assignment for L', χ, N under the two gauge groups of $[U(1)_Y, U(1)_H]$ are $(-1/2, 2x)$, $(0, x)$, and $(0, y)$, respectively. Here, we use two arbitrary integers (x, y) with $\{x, y\} \neq 0$ to keep track of the heavy fermions running in the outer and inner loops of the neutrino mass diagram (see Fig. 1). As for new scalar fields, we introduce four inert scalar fields s, η, s', η', where (η, η') are $SU(2)_L$ doublets and (s, s') are singlets. We can see that, since (s, η) are charged under the $U(1)_H$ as $(-2x, x)$, these two fields will only interact with new fermions of L' and χ. On the other hand, the two prime fields (s', η') are charged with $(x + y, -2x + y)$ for the hidden symmetry; thus, they are allowed to connect with the exotic fermion N under the assumption of $y \neq -x$, $y \neq 2x$.[1] The two scalar fields (H, φ) are needed in order to generate the neutrino mass at the two-loop level, provided they mix inert scalars (η, s) and (η', s') inside each set. The symmetry permits more scalar fields, like a doublet H' or a triplet Δ, to induce the $Z - Z'$ mixing for the LHC collider signature. In the case of adding H', the neutrino mass will be generated at the one-loop level since the red dot in Fig. 1 can be substituted by an interaction of $\overline{L'^c}_{L/R} H' \chi_{L/R}$. However, in such case, the VEV of H' should be very small (equivalent to loop generated), so this one-loop radiative seesaw mechanism may be able to reconcile the tension between the neutrino mass and the relic density bound. Thus, we focus on exploring the impact of a triplet Δ interplaying with (H, φ) via the scalar potential in the two-loop radiative seesaw mechanism. For that purpose, the scalars H, Δ, and φ are required to develop nonzero VEVs, respectively symbolized by $\langle H \rangle \equiv v_H/\sqrt{2}$, $\langle \Delta \rangle \equiv v_\Delta/\sqrt{2}$, $\langle \varphi \rangle \equiv v_\varphi/\sqrt{2}$. The valid renormalizable Lagrangian for the fermion sector is given by

$$
\begin{aligned}
-\mathcal{L}_Y = {} & y_{\ell_{ii}} \bar{L}_{L_i} H e_{R_i} + y^L_{\chi_{ab}} s \bar{\chi}^c_{L_a} \chi_{L_b} + y^R_{\chi_{ab}} s \bar{\chi}^c_{R_a} \chi_{R_b} \\
& + y_{\eta_{ia}} \bar{L}_{L_i} \tilde{\eta} \chi_{R_a} + y_{S_{ia}} s \bar{L}_{L_i} L'_{R_a} + y_{\eta'_{ab}} \bar{L}'_{R_a} \tilde{\eta}' N_{L_b} \\
& + y'_{\eta'_{ab}} \bar{L}'_{L_a} \tilde{\eta}' N_{R_b} + y_{s'_{ab}} \bar{N}_{R_a} \chi^c_{R_b} s' + y'_{s'_{ab}} \bar{N}_{L_a} \chi^c_{L_b} s' \\
& + M_{\chi_{aa}} \bar{\chi}_{L_a} \chi_{R_a} + M_{N_{aa}} \bar{N}_{L_a} N_{R_a} + M_{N'_{aa}} \bar{L}'_{L_a} L'_{R_a} \\
& + \text{H.c.},
\end{aligned} \tag{2.1}
$$

[1] In fact, we can see that the gauged $U(1)_H$ is a linear combination of two global $U(1)$s, which should be observed individually in the unbroken phase.
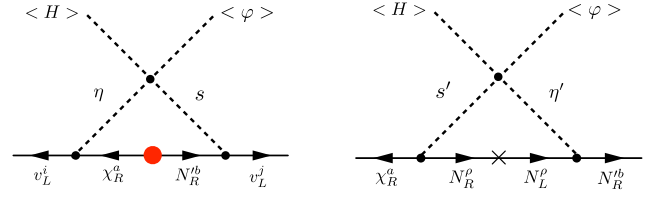

FIG. 1. Neutrino mass in the gauge basis at the two-loop level, where the right plot represents the red dot in the left plot.

where $i, a, b = 1, 2, 3$ are the flavor indices for the SM and exotic fermions, and $\tilde{\eta} \equiv i\sigma_2\eta^*$, with σ_2 being the second Pauli matrix. For simplicity, we assume that all coefficients are real and M_χ, M_N, $M_{N'}$ are diagonal matrices. The first term of $\mathcal{L}_Y$ generates the SM charged-lepton masses $m_{\ell_i} \equiv y_{\ell_i} v_H/\sqrt{2}$, while the second to fourth terms are responsible for the (semi)annihilations. The residual $\mathbb{Z}_3$ from the broken hidden symmetry makes the lightest neutral states, with $U(1)_H$ charge of x or $\pm 2x$, i.e., particles in the set of (χ_i, N'_i, η, s), our DM candidate. In this paper we are interested in the mass pattern where χ_1 actually plays the role of DM. Referring to Table I, we can see that the two scalar fields (Δ, φ) carry a $U(1)_H$ charge $q_H = -3x$ with $x \in$ integer, so they will transform under the Abelian $U(1)$ symmetry as $\Delta \to e^{-iq_H\alpha}\Delta$ and $\varphi \to e^{-iq_H\alpha}\varphi$, for an arbitrary value of α before the spontaneous symmetry breaking. However, after these two scalars obtain VEVs, the phase is forced to be $\alpha = 2\pi/3$ for any integer $x \geq 1$; thus the Lagrangian is still invariant under a discrete $\mathbb{Z}_3$ symmetry. The particles with $x(2x)$ charge in $U(1)_H$ have $w = e^{i2\pi/3}(w^2)$ parity assignment under this $\mathbb{Z}_3$.

A. The scalar potential

We explicitly write the nontrivial terms for the inert scalar potential, which are invariant under the $SU(2)_L \times U(1)_Y \times U(1)_H$ gauge symmetry:

$$
\begin{aligned}
\mathcal{V}_1 = {} & (\lambda_0 H^\dagger \eta s^* \varphi + \lambda'_0 H^\dagger \eta' s'^* \varphi^* + \text{H.c.}) \\
& + \sum_\phi^{\eta, \eta', s, s'} [\lambda_{H\phi}(H^\dagger H)(\phi^\dagger \phi) + \lambda_{\varphi\phi}(\varphi^\dagger \varphi)(\phi^\dagger \phi)] \\
& + \sum_\phi^{\eta, \eta'} \lambda'_{H\phi}(H^\dagger \phi)(\phi^\dagger H) + \sum_\phi^{\eta, \eta', s, s'} [\mu_\phi^2 \phi^\dagger \phi + \lambda_\phi |\phi^\dagger \phi|^2],
\end{aligned} \tag{2.2}
$$

where we assume that these terms, like $s'^2\varphi^{(*)}$, $s'^2\varphi^2$, $\eta'^\dagger\eta\varphi^2$, vanish due to $U(1)_H$ charges (e.g., $x = y = 1$). Thus, no mass splitting occurs among the real and imaginary parts of any inert field. The general potential for the scalars (H, Δ) can be found in Refs. [21,22], and we will modify it by adding interactions with a complex singlet φ,

TABLE I.   Contents of fermion and scalar fields and their charge assignments under $SU(2)_L \times U(1)_Y \times U(1)_H$, where all the new fields are singlets under $SU(3)_C$ and all the quark fields are neutral under $U(1)_H$. Note that the H' field is only present for the one-loop radiative seesaw mechanism.

	Fermion fields					Scalar fields				Inert scalar fields			
	L_L	e_R	$L'_{L/R}$	$\chi_{L/R}$	$N_{L/R}$	H	H'	Δ	φ	s	η	s'	η'
$SU(2)_L$	2	1	2	1	1	2	2	3	1	1	2	1	2
$U(1)_Y$	$-\frac{1}{2}$	-1	$-\frac{1}{2}$	0	0	$\frac{1}{2}$	$\frac{1}{2}$	1	0	0	$\frac{1}{2}$	0	$\frac{1}{2}$
$U(1)_H$	0	0	$2x$	x	y	0	$-3x$	$-3x$	$-3x$	$-2x$	x	$x+y$	$-2x+y$

$$
\begin{aligned}
\mathcal{V}_2 = {}& -\mu_H^2 H^\dagger H + \lambda_H (H^\dagger H)^2 + M^2 Tr(\Delta^\dagger \Delta) \\
& + \lambda_1 (Tr(\Delta^\dagger \Delta))^2 + \lambda_2 Tr((\Delta^\dagger \Delta)^2) \\
& + \lambda_3 (H^\dagger H) Tr(\Delta^\dagger \Delta) + \lambda_4 H^\dagger \Delta \Delta^\dagger H - \mu_\varphi^2 \varphi^* \varphi \\
& + \lambda_\varphi (\varphi^* \varphi)^2 + \lambda_5 H^\dagger H \varphi^* \varphi + \lambda_6 Tr(\Delta^\dagger \Delta) \varphi^* \varphi \\
& + [\lambda_\Delta H^T i\sigma_2 \Delta^+ H \varphi + \text{H.c.}].
\end{aligned} \tag{2.3}
$$

The scalar fields, besides the inert ones, are explicitly expressed as

$$
H = \begin{bmatrix} G^+ \\ \frac{v_H + h + iG^0}{\sqrt{2}} \end{bmatrix}, \qquad
\Delta = \begin{bmatrix} \frac{\Delta^+}{\sqrt{2}} & \Delta^{++} \\ \frac{v_\Delta + \Delta_R + i\Delta_I}{\sqrt{2}} & -\frac{\Delta^+}{\sqrt{2}} \end{bmatrix},
$$

$$
\varphi = \frac{v_\varphi + \varphi_R + i\varphi_I}{\sqrt{2}}, \tag{2.4}
$$

so the mass of the W boson is fixed to $m_W = \frac{g_2 \sqrt{v_H^2 + 2v_\Delta^2}}{2}$. The minimum of the potential is determined by derivatives $\partial \mathcal{V}_2 / \partial v_H = 0$, $\partial \mathcal{V}_2 / \partial v_\Delta = 0$, $\partial \mathcal{V}_2 / \partial v_\varphi = 0$, which read as

$$
-\mu_H^2 + \lambda_H v_H^2 + \frac{\lambda_3 + \lambda_4}{2} v_\Delta^2 + \frac{\lambda_5}{2} v_\varphi^2 = \lambda_\Delta v_\Delta v_\varphi
$$

$$
\left(M^2 + \frac{\lambda_3 + \lambda_4}{2} v_H^2 + (\lambda_1 + \lambda_2) v_\Delta^2 + \frac{\lambda_6}{2} v_\varphi^2 \right) v_\Delta = \lambda_\Delta v_H^2 v_\varphi / 2
$$

$$
\left(-\mu_\varphi^2 + \lambda_\varphi v_\varphi^2 + \frac{\lambda_5}{2} v_H^2 + + \frac{\lambda_6}{2} v_\Delta^2 \right) v_\varphi = \lambda_\Delta v_H^2 v_\Delta / 2.
$$
$$\tag{2.5}$$

As we argue in Sec. II D for $Z - Z'$ mixing, v_Δ is very tiny due to the ρ parameter; thus we focus on the limit of $v_\Delta \ll v_H \lesssim v_\varphi$. Under the assumption of negligible mixing between φ and (H, Δ), i.e., $\lambda_5, \lambda_6 \ll 1$, we obtain

$$
v_H \simeq \left(\frac{\lambda_\Delta v_\Delta v_\varphi + \mu_H^2}{\lambda_H} \right)^{1/2}, \quad v_\Delta \simeq \frac{\lambda_\Delta v_H^2 v_\varphi}{2(M^2 + (\lambda_3 + \lambda_4) v_H^2 / 2)},
$$

$$
v_\varphi \simeq \frac{\mu_\varphi}{\lambda_\varphi^{1/2}}. \tag{2.6}
$$

In addition, the mass matrices in terms of (h, Δ_R, φ_R), $(G^0, \Delta_I, \varphi_I)$, and (G^+, Δ^+) can be diagonalized into a CP-even or odd spectrum by respective orthogonal matrices. Analogously, the inert bosons $(s, \eta)_{R/I}$ and $(s', \eta')_{R/I}$ are written as

$$
\eta = \begin{bmatrix} \eta^+ \\ \frac{\eta_R + i\eta_I}{\sqrt{2}} \end{bmatrix}, \qquad s = \frac{s_R + i s_I}{\sqrt{2}};
$$

$$
\eta' = \begin{bmatrix} \eta'^+ \\ \frac{\eta'_R + i\eta'_I}{\sqrt{2}} \end{bmatrix}, \qquad s' = \frac{s'_R + i s'_I}{\sqrt{2}}. \tag{2.7}
$$

They are rotated into the mass basis as follows:

$$
V_\alpha^T \begin{bmatrix} m_{s_R}^2 & \frac{\lambda_0}{2} v_H v_\varphi \\ \frac{\lambda_0}{2} v_H v_\varphi & m_{\eta_R}^2 \end{bmatrix} V_\alpha = \begin{bmatrix} m_{H_1}^2 & 0 \\ 0 & m_{H_2}^2 \end{bmatrix},
$$

$$
V_{\alpha'}^T \begin{bmatrix} m_{s'_R}^2 & \frac{\lambda'_0}{2} v_H v_\varphi \\ \frac{\lambda'_0}{2} v_H v_\varphi & m_{\eta'_R}^2 \end{bmatrix} V_{\alpha'} = \begin{bmatrix} m_{H'_1}^2 & 0 \\ 0 & m_{H'_2}^2 \end{bmatrix} \tag{2.8}
$$

$$
\begin{bmatrix} s_R + i s_I \\ \eta_R + i\eta_I \end{bmatrix} = \begin{bmatrix} c_\alpha & -s_\alpha \\ s_\alpha & c_\alpha \end{bmatrix} \begin{bmatrix} H_1 + iA_1 \\ H_2 + iA_2 \end{bmatrix},
$$

$$
\begin{bmatrix} s'_R + i s'_I \\ \eta'_R + i\eta'_I \end{bmatrix} = \begin{bmatrix} c_{\alpha'} & -s_{\alpha'} \\ s_{\alpha'} & c_{\alpha'} \end{bmatrix} \begin{bmatrix} H'_1 + iA'_1 \\ H'_2 + iA'_2 \end{bmatrix} \tag{2.9}
$$

where we use short-hand notation of $s_{\alpha^{(')}} = \sin\alpha^{(')}$, $c_{\alpha^{(')}} = \cos\alpha^{(')}$ and the complex fields $H_i + iA_i$, $H'_i + iA'_i$, $i = 1, 2$ are mass eigenstates. Note that the semiannihilation exists for the theory with $\mathbb{Z}_3$ parity, indicating that we need to keep the degeneracy between $H_{1,(2)}$ and $A_{1,(2)}$. The reason is that a $\mathbb{Z}_3$ parity assignment $w = e^{i2\pi/3}$ is valid for a Dirac fermion or a complex scalar field, like $\tilde{H}_i = H_i + iA_i$ with $i = 1, 2$. Under this specific potential we obtain $m_{H_{1,2}}^2 = m_{A_{1,2}}^2$, $m_{H'_{1,2}}^2 = m_{A'_{1,2}}^2$. Without loss of generality, we can assume $m_{H_1} < m_{H_2}$ and $m_{H'_1} < m_{H'_2}$ by ordering the mass eigenstates.
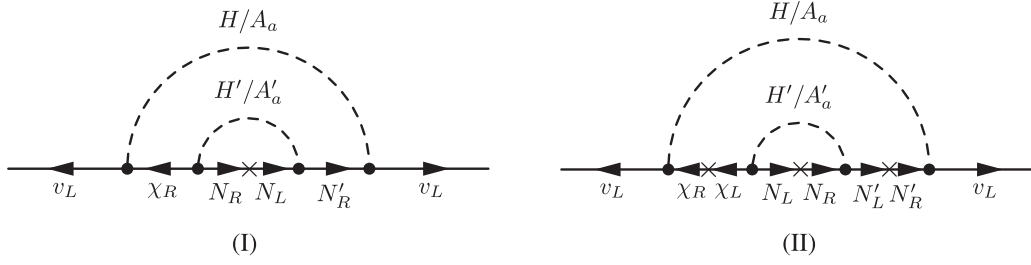
FIG. 2. The Feynman diagrams for neutrino masses generated at the two-loop level in the mass eigenstate basis of inert scalars.

B. Neutrino mass matrix

In this model, the neutrino mass arises at the two-loop level. To facilitate the calculation, the Lagrangian should be transformed into the mass basis:

$$
\begin{aligned}
-\mathcal{L}_Y \sim{} & \frac{y_{\eta_{ia}}}{\sqrt{2}} \bar{\nu}_{L_i} \chi_{R_a}(s_\alpha H_1 + c_\alpha H_2) - i \frac{y_{\eta_{ia}}}{\sqrt{2}} \bar{\nu}_{L_i} \chi_{R_a}(s_\alpha A_1 + c_\alpha A_2) \\
& + \frac{y^{L/R}_{\chi_{ab}}}{\sqrt{2}} \bar{\chi}^C_{L_a/R_a} \chi_{L_a/R_b}(c_\alpha H_1 - s_\alpha H_2) + i \frac{y^{L/R}_{\chi_{ab}}}{\sqrt{2}} \bar{\chi}^C_{L_a/R_a} \chi_{L_a/R_b}(c_\alpha A_1 - s_\alpha A_2) \\
& + \frac{y_{S_{ia}}}{\sqrt{2}} \bar{\nu}_{L_i} N'_{R_a}(c_\alpha H_1 - s_\alpha H_2) + i \frac{y_{S_{ia}}}{\sqrt{2}} \bar{\nu}_{L_i} N'_{R_a}(c_\alpha A_1 - s_\alpha A_2) \\
& + \frac{y_{s'_{ab}}}{\sqrt{2}} \bar{N}_{R_a} \chi^C_{R_b}(c_{\alpha'} H'_1 - s_{\alpha'} H'_2) + i \frac{y_{s'_{ab}}}{\sqrt{2}} \bar{N}_{R_a} \chi^C_{R_b}(c_{\alpha'} A'_1 - s_{\alpha'} A'_2) \\
& + \frac{y'_{s'_{ab}}}{\sqrt{2}} \bar{N}_{L_a} \chi^C_{L_b}(c_{\alpha'} H'_1 - s_{\alpha'} H'_2) + i \frac{y'_{s'_{ab}}}{\sqrt{2}} \bar{N}_{L_a} \chi^C_{L_b}(c_{\alpha'} A'_1 - s_{\alpha'} A'_2) \\
& + \frac{y_{\eta'_{ab}}}{\sqrt{2}} \bar{N}'_{R_a} N_{L_b}(s_{\alpha'} H'_1 + c_{\alpha'} H'_2) - i \frac{y_{\eta'_{ab}}}{\sqrt{2}} \bar{N}'_{R_a} N_{L_b}(s_{\alpha'} A'_1 + c_{\alpha'} A'_2) \\
& + \frac{y'_{\eta'_{ab}}}{\sqrt{2}} \bar{N}'_{L_a} N_{R_b}(s_{\alpha'} H'_1 + c_{\alpha'} H'_2) - i \frac{y'_{\eta'_{ab}}}{\sqrt{2}} \bar{N}'_{L_a} N_{R_b}(s_{\alpha'} A'_1 + c_{\alpha'} A'_2) + \text{H.c.}
\end{aligned}
\tag{2.10}
$$

Here we assume that all the Yukawa couplings are real for simplicity. The active neutrino mass matrix $m_{\nu_{ij}}$ is generated at two-loop level as shown in Fig. 2, with formulas given by

$$
(m_\nu)_{ij} = m^{(I)}_{\nu_{ij}} + m^{(II)}_{\nu_{ij}} + [m^{(I)}_{\nu_{ij}}]^T + [m^{(II)}_{\nu_{ij}}]^T,
\tag{2.11}
$$

where $m^{(I)}_{\nu_{ab}}$ and $m^{(II)}_{\nu_{ab}}$, respectively, correspond to the left and right plots in Fig. 2. The constraint on the neutrino matrix is from the neutrino oscillation data since $(m_\nu)_{ab}$ has to be diagonalized by the Pontecorvo-Maki-Nakagawa-Sakata mixing matrix V_{MNS} (PMNS) [23] as $(m_\nu)_{ij} = (V^*_{\text{MNS}} D_\nu V^\dagger_{\text{MNS}})_{ij}$ with $D_\nu = \text{diag}(m_{\nu_1}, m_{\nu_2}, m_{\nu_3})$. The PMNS matrix is parametrized as

$$
V_{\text{MNS}} = \begin{bmatrix} c_{13}c_{12} & c_{13}s_{12} & s_{13}e^{-i\delta} \\ -c_{23}s_{12} - s_{23}s_{13}c_{12}e^{i\delta} & c_{23}c_{12} - s_{23}s_{13}s_{12}e^{i\delta} & s_{23}c_{13} \\ s_{23}s_{12} - c_{23}s_{13}c_{12}e^{i\delta} & -s_{23}c_{12} - c_{23}s_{13}s_{12}e^{i\delta} & c_{23}c_{13} \end{bmatrix} \text{diag}(1, e^{i\frac{\alpha_{21}}{2}}, e^{i\frac{\alpha_{31}}{2}})
\tag{2.12}
$$

with $s_{ij} = \sin\theta_{ij}$ being three mixing angles. In the following analysis, we also neglect the Majorana CP violation phase α_{21} and α_{31} as well as the Dirac CP violation phase δ. By assuming the normal mass order $m_{\nu 1} \ll m_{\nu 2} < m_{\nu 3}$, the global fit of the current experiments at 3σ is given by [24]
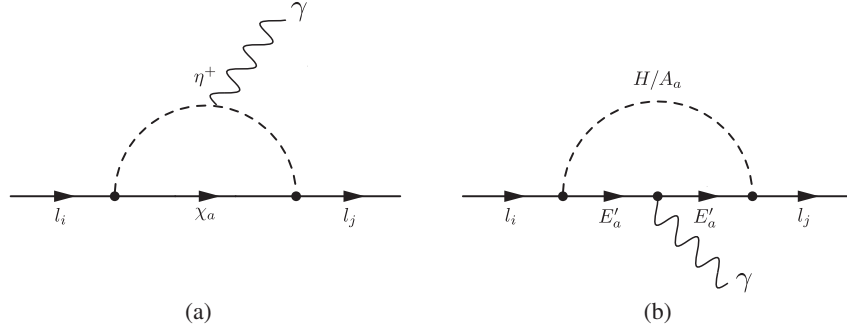
FIG. 3.   Lepton flavor violation processes induced by heavy fermions and scalars.

$$0.250 \leq s_{12}^2 \leq 0.354, \qquad 0.381 \leq s_{23}^2 \leq 0.615,$$

$$0.019 \leq s_{13}^2 \leq 0.024,$$

$$m_{\nu_3}^2 - m_{\nu_1}^2 = (2.45\text{–}2.69) \times 10^{-3} \text{ eV}^2,$$

$$m_{\nu_2}^2 - m_{\nu_1}^2 = (6.93\text{–}7.96) \times 10^{-5} \text{ eV}^2. \tag{2.13}$$

Now we rewrite the neutrino mass matrix in terms of Yukawa couplings and the form factors:

$$(m_\nu)_{ij} \equiv \frac{1}{(4\pi)^4} (y_{\eta_{ia}}[F_I + F_{II}]_{ab} y_{S_{bj}}^T + y_{S_{ja}}[F_I^T + F_{II}^T]_{ab} y_{\eta_{bj}}^T)$$

$$\equiv \frac{1}{(4\pi)^4} (y_{\eta_{ia}} G_{ab} y_{S_{bj}}^T + y_{S_{ja}} G_{ab}^T y_{\eta_{bj}}^T), \tag{2.14}$$

where the factor $\frac{1}{(4\pi)^4}$ comes from the loop integration and the exact expressions for these form factors F_I, F_{II} can be found in Appendix A. The form factors exhibit an interesting property, proportional to the product of mass differences $(m_{H_2}^2 - m_{H_1}^2)(m_{H_2'}^2 - m_{H_1'}^2)$. Thus the neutrino mass can be easily accommodated in the sub-eV order if either set of inert scalars is quasidegenerate without tuning the Yukawa couplings. In particular, if we set $m_{H_1'} \simeq m_{H_2'}$, the LFV bound will not be influenced as $H_{1,2}'$ do not mediate these processes.

Because of the symmetric property, Eq. (2.14) can be conveniently recast into a suitable form for the numerical analysis:

$$y_\eta = \frac{1}{2}[(V_{\text{MNS}}^* D_\nu V_{\text{MNS}}^\dagger + A)(y_S^T)^{-1} G^{-1}, \tag{2.15}$$

where the A is an arbitrary antisymmetric matrix on the order $\lesssim 10^{-9}$ and of complex values if there is CP violation [25]. Therefore, after we impose Eq. (2.15), the y_η coupling is no longer a free parameter but a function of y_S and the neutrino mass form factors. This parameter will be determined by the neutrino oscillation data up to an uncertainty. Notice that $y_\eta \lesssim \sqrt{4\pi}$ should be satisfied in the perturbative limit.

C. LFV and muon $g-2$

In this radiative neutrino mass model, the existence of charged scalars and vectorlike fermions contributes to lepton flavor violation processes (see Fig. 3), which in turn will severely constrain the Yukawa couplings and masses of heavy scalars and fermions. The relevant Lagrangian for LFV can be expressed as

$$\mathcal{L} = -y_{\eta_{ia}} \bar{\ell}_{L_i} \eta^- \chi_{R_a} + \frac{1}{\sqrt{2}} y_{S_{ia}} \bar{\ell}_{L_i} E_{R_a}' [(c_{\alpha_R} H_1 - s_{\alpha_R} H_2)$$

$$+ i(c_{\alpha_I} A_1 - s_{\alpha_I} A_2)] + \text{H.c.} \tag{2.16}$$

We can calculate the branching ratio for the LFV decay process $\ell_i \to \ell_j \gamma$ in terms of amplitude $a_{L/R}$, which encodes the loop integration of the Feynman diagrams:

$$\text{Br}(\ell_i \to \ell_j \gamma) \approx \frac{48\pi^3 \alpha_{\text{em}}}{G_F^2 m_{\ell_i}^2} C_{ij}(|a_{L_{ij}}|^2 + |a_{R_{ij}}|^2), \tag{2.17}$$

where $G_F \approx 1.166 \times 10^{-5} \text{ GeV}^{-2}$ is the Fermi constant, $\alpha_{\text{em}}(m_Z) \approx 1/128.9$ is the fine-structure constant [24], $C_{21} \approx 1$, $C_{31} \approx 0.1784$, and $C_{32} \approx 0.1736$. In this specific model a_R is formulated as

$$a_{R_{ij}} \approx \frac{m_{\ell_i}}{(4\pi)^2} [y_{\eta_{ja}} y_{\eta_{ai}}^\dagger H(\chi_a, \eta^-)$$

$$- \frac{y_{S_{ja}} y_{S_{ai}}^\dagger}{2} [c_{\alpha_R}^2 H(H_1, E_a') + s_{\alpha_R}^2 H(H_2, E_a')$$

$$+ c_{\alpha_I}^2 H(A_1, E_a') + s_{\alpha_I}^2 H(A_2, E_a')]], \tag{2.18}$$

$$H(a, b)$$

$$= \int_0^1 dx \int_0^{1-x} dy \frac{xy}{xm_a^2 + (1-x)m_b^2}$$

$$\overset{m_a \neq m_b}{=\!=} \frac{2m_a^6 + 3m_a^4 m_b^2 - 6m_a^2 m_b^4 + m_b^6 + 6m_a^4 m_b^2 \log(\frac{m_b^2}{m_a^2})}{12(m_a^2 - m_b^2)^4}$$

$$\tag{2.19}$$

where we can see that the loop contributions from two resources [Figs. 2(a) and 2(b)] are of opposite sign. And for

the left-handed amplitude, a_L is obtained by a mass substitution: $a_L = a_R(m_{\ell_i} \to m_{\ell_j})$.

The couplings involved in those LFV processes are y_η and y_S, which are strongly correlated with the neutrino mass matrix. In particular, the magnitude of y_η, along with the masses m_{χ_1} and $m_{H_{1,2}}$, constrained by the LFV bound, will influence the DM relic density as well. To find the allowed parameter space for this model, the following upper bounds are imposed [26,27],

$$\mathrm{Br}(\mu \to e\gamma) \leq 4.2 \times 10^{-13}(6 \times 10^{-14})$$
$$\mathrm{Br}(\tau \to \mu\gamma) \leq 4.4 \times 10^{-8}, \qquad \mathrm{Br}(\tau \to e\gamma) \leq 3.3 \times 10^{-8}$$
$$(2.20)$$

where the upper bound from $\mu \to e\gamma$ is the most stringent one, with the value in parentheses indicating a future reach of the MEG experiment [28].

The muon anomalous magnetic moment.—The muon $g - 2$ is a well-measured property, and a large 3.6σ discrepancy of Δa_μ between the SM theory and experimental measurement was observed for a long time. For this model, one can estimate the muon $g - 2$ through the amplitudes formulated above:

$$\Delta a_\mu \approx -m_\mu(a_L + a_R)_{22}. \qquad (2.21)$$

The deviation from the SM prediction is $\Delta a_\mu = a_\mu^{\mathrm{exp}} - a_\mu^{\mathrm{SM}} = (2.74 \pm 0.73) \times 10^{-9}$ [24] with a positive value. However, because our analysis shows that the muon $g - 2$ is too tiny after imposing other bounds, we just employ the muon $g - 2$ as a model quality for reference.

D. $Z - Z'$ mixing

The effect of the hidden Z' at the TeV scale will actually decouple from the dark matter physics, and we would like to qualify this argument in this section. After the three scalar fields develop VEVs, $U(1)_H$ and electroweak symmetries are spontaneously broken so that the mass terms of the neutral gauge boson are obtained,

$$\frac{1}{2}\begin{pmatrix} Z_0 \\ \tilde{Z} \end{pmatrix}^T \begin{bmatrix} \frac{(g_1^2+g_2^2)}{4}(v_H^2 + 4v_\Delta^2) & 3x\sqrt{g_1^2 + g_2^2}g_H v_\Delta^2 \\ 3x\sqrt{g_1^2 + g_2^2}g_H v_\Delta^2 & 9x^2g_H^2(v_\Delta^2 + v_\varphi^2) \end{bmatrix}\begin{pmatrix} Z_0 \\ \tilde{Z} \end{pmatrix},$$
$$(2.22)$$

where g_2, g_1, and g_H are gauge couplings of $SU(2)_L$, $U(1)_Y$, and $U(1)_H$, respectively. The Z_0 and $\tilde{Z}$ are the gauge fields for $U(1)_Y$ and $U(1)_H$ with the Z_0 mostly composed of the SM Z boson. Here we assume that the kinetic mixing between the two Abelian gauge bosons is negligibly small for simplicity. In the case of $x = 1$, we parametrize the mass matrix to be

$$\begin{bmatrix} \frac{(g_1^2+g_2^2)}{4}(v_H^2 + 4v_\Delta^2) & 3\sqrt{g_1^2 + g_2^2}g_H v_\Delta^2 \\ 3\sqrt{g_1^2 + g_2^2}g_H v_\Delta^2 & 9g_H^2(v_\Delta^2 + v_\varphi^2) \end{bmatrix}$$
$$= m_{\tilde{Z}}^2 \begin{bmatrix} \epsilon_1^2 & 2\epsilon_1\epsilon_2\epsilon_3 \\ 2\epsilon_1\epsilon_2\epsilon_3 & 1 + \epsilon_2^2 \end{bmatrix}, \qquad (2.23)$$

where we use the definition of $m_{Z_0} = \frac{\sqrt{(g_1^2+g_2^2)(v_H^2+4v_\Delta^2)}}{2}$, $m_{\tilde{Z}} = 3g_H v_\varphi$, $\epsilon_1 = \frac{m_{Z_0}}{m_{\tilde{Z}}}$ and $\epsilon_2 = \frac{v_\Delta}{v_\varphi}$, $\epsilon_3 = \frac{v_\Delta}{\sqrt{v_H^2+4v_\Delta^2}}$. The mass matrix can be diagonalized by an orthogonal transformation to be $\mathrm{Diag}(m_Z^2, m_{Z'}^2)$, and in an approximation of $v_\Delta \ll v_H \lesssim v_\varphi$ and $g_H = \mathcal{O}(1)$, this gives

$$m_Z^2 \approx m_{Z_0}^2(1 - 4\epsilon_2^2\epsilon_3^2), \qquad m_{Z'}^2 \approx m_{\tilde{Z}}^2(1 + \epsilon_2^2), \quad (2.24)$$

$$\begin{pmatrix} Z \\ Z' \end{pmatrix} = \begin{bmatrix} c_Z & s_Z \\ -s_Z & c_Z \end{bmatrix}\begin{pmatrix} Z_0 \\ \tilde{Z} \end{pmatrix}, \qquad \tan\theta_Z = \frac{-2\epsilon_1\epsilon_2\epsilon_3}{1 + \epsilon_2^2 - \epsilon_1^2}.$$
$$(2.25)$$

If we fix $c_W^2 = g_2^2/(g_1^2 + g_2^2)$ as the SM value, the ρ parameter can be expressed as

$$\rho_0 \simeq \frac{(1 + \frac{2v_\Delta^2}{v_H^2})}{(1 + \frac{4v_\Delta^2}{v_H^2})(1 - 4\epsilon_2^2\epsilon_3^2)}. \qquad (2.26)$$

The experimental constraint from the PDG is $\rho_{0,\mathrm{exp}} = 1.00039 \pm 0.00019$ [24], which will translate into a requirement of $v_\Delta \lesssim 3.5$ GeV. In this paper, we assume the Z' boson mass to be above the TeV scale for $v_\varphi \gtrsim 350$ GeV. According to Eq. (2.25), this results in an extremely small $|\tan\theta_Z| < 10^{-5}$ compared with the Yukawa coupling with DM and the neutrino. Thus as long as we prefer the DM mass in $\mathcal{O}(100)$ GeV, it will be safe to neglect the impact of Z' on either DM annihilation or DM-nucleon scattering.

E. Bound of electroweak precision test

The electroweak precision test (EWPT) on low energy observables can set limits for deviations from the SM. The new physics effects are mainly encoded in the oblique parameters S, T, and U, expressed in terms of the transverse part of the gauge boson's self-energy amplitudes. For this model, since the U parameter is suppressed by an additional factor of v^2/M_{new}^2, its effect is neglected. Due to the vectorlike nature and degeneracy, the exotic particles of L_i' have no impact on oblique parameters, i.e., $\Delta S_f = \frac{2}{3\pi}(t_{3L} - t_{3R})^2 = 0$ and $\Delta T_f = 0$ [24]. However, the inert scalars (η, s) may cause notable deviation to $S = -16\pi\Pi'(0)_{W_3B}$ and $T = \frac{4\pi}{m_Z^2 s_W^2 c_W^2}[2\Pi_{W_1W_1}(0) - \Pi_{W_3W_3}(0)]$ [29]; we will discuss their constraints on the mass splitting among (m_{η^+}, m_{H_i}) and the mixing angle $\sin(\alpha)$. After evaluating
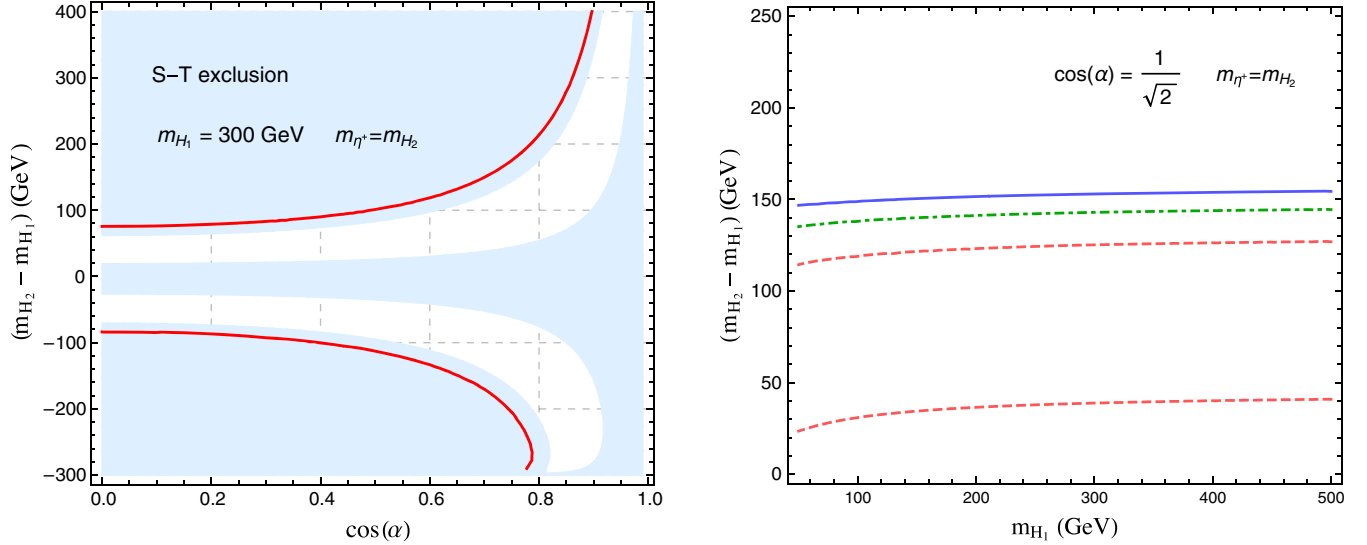
FIG. 4.   In the left plot, the two white bands represent the region allowed by the $S - T$ bound at the 1σ C.L., while the red line is the 3σ bound for $m_{H_2} = 300$ GeV. The right plot shows the bound for $(m_{H_2} - m_{H_1})$ and m_{H_1} in the case of $s_\alpha = c_\alpha = \frac{1}{\sqrt{2}}$ (assuming $m_{H_2} > m_{H_1}$ and $m_{\eta^+} = m_{H_2}$), where the regions outside the contours of the red, green, and blue lines are excluded at 68% (1σ), 95% (2σ), and 99% (3σ) C.L.s.

the relevant self-energy correlations, we find that the effects from the inert scalars are described by

$$
\Delta S = \frac{1}{12\pi}[s_\alpha^4 G(m_{H_1}, m_{H_1}, m_{\eta^+}) + c_\alpha^4 G(m_{H_2} m_{H_2}, m_{\eta^+})
$$
$$
+ 2c_\alpha^2 s_\alpha^2 G(m_{H_1}, m_{H_2}, m_{\eta^+})]
$$
$$
= \frac{1}{12\pi}\left[s_\alpha^2 \ln\left(\frac{m_{H_1}^2}{m_{\eta^+}^2}\right) + c_\alpha^2 \ln\left(\frac{m_{H_2}^2}{m_{\eta^+}^2}\right) \right.
$$
$$
\left. - 3c_\alpha^2 s_\alpha^2 \chi(m_{H_1}, m_{H_2}) \right], \tag{2.27}
$$

$$
\Delta T = \frac{1}{16\pi m_W^2 s_W^2}[s_\alpha^2 F(m_{H_1}, m_{\eta^+}) + c_\alpha^2 F(m_{H_2} m_{\eta^+})
$$
$$
- c_\alpha^2 s_\alpha^2 F(m_{H_1}, m_{H_2})], \tag{2.28}
$$

where the loop functions $G(m_1, m_2, m_3)$, $\chi(m_1, m_2)$, and $F(m_1, m_2)$ are defined as

$$
G(m_1, m_2, m_3) = \frac{1}{2}\left[\ln\left(\frac{m_1^2 m_2^2}{m_3^4}\right) - 3\chi(m_1, m_2) \right], \tag{2.29}
$$

$$
\chi(m_1, m_2) = \frac{5(m_1^4 + m_2^4) - 22m_1^2 m_2^2}{9(m_1^2 - m_2^2)^2}
$$
$$
+ \frac{3m_1^2 m_2^2(m_1^2 + m_2^2) - m_1^6 - m_2^6}{3(m_1^2 - m_2^2)^3}\ln\left(\frac{m_1^2}{m_2^2}\right), \tag{2.30}
$$

$$
F(m_1, m_2) = m_1^2 + m_2^2 - \frac{2m_1^2 m_2^2}{m_1^2 - m_2^2}\ln\left(\frac{m_1^2}{m_2^2}\right), \tag{2.31}
$$

with $\chi(m_1, m_2)$ and $F(m_1, m_2)$ being symmetric for $m_1 \leftrightarrow m_2$ and vanishing for equal masses, i.e., $\chi(m, m) = F(m, m) = 0$. During the calculation, the divergences inherent in the two-point functions are properly canceled.[2] In the case of the SM Higgs h barely mixing with (Δ, φ), the ΔT is exactly the wave-function renormalization of the Goldstone bosons G^+, G^0 with $(\eta^\pm, ((\eta_R + i\eta_I)/\sqrt{2}), s)$ running inside the loops (refer to Appendix B for details) [31]. However, for the ΔS, the function $G(m_1, m_2, m_3)$ is related to $\frac{d}{dp^2}[B_{22}(p^2, m_1^2, m_2^2) - B_{22}(p^2, m_3^2, m_3^2)]|_{p^2=0} = \frac{1}{2}\int_0^1 dx x(1-x)\ln[\frac{xm_1^2 + (1-x)m_2^2}{m_3^2}]$, using the Passarino-Veltman function B_{22} defined in [32].

The bound for the S and T parameters is obtained from the precision electroweak data, such as M_Z and Γ_Z, at the 1σ deviation by fixing $U = 0$ [24]:

$$
S = 0.02 \pm 0.07 \qquad T = 0.06 \pm 0.06 \tag{2.32}
$$

with an off-diagonal correlation of 92%. In Fig. 4, combining all the discussed parts, we translate the S-T χ^2 fit into the bounds of inert scalar masses and the mixing angle. Since both ΔS and ΔT are symmetric functions of

---

[2]For the T parameter, if we calculate it in terms of the gauge boson's self-energy amplitudes, the divergence is fully captured in the loop function $A_0(m^2) = \frac{1}{i\pi^2}\int \frac{d^4k}{(k^2 - m^2)}$ [30] and should be canceled after counting all the diagrams. The cancellation due to the mixing of neutral inert scalars $((\eta_R + i\eta_I)/\sqrt{2}), s)$ [precisely speaking, $(H_{1,2}, A_{1,2})$ in the mass basis] is demonstrated by the following pattern: $2s_\alpha^2 A_0(m_{H_1}^2) + 2c_\alpha^2 A_0(m_{H_2}^2) - 2s_\alpha^4 A_0(m_{H_1}^2) - 2c_\alpha^4 A_0(m_{H_2}^2) - 2c_\alpha^2 s_\alpha^2(A_0(m_{H_1}^2) + A_0(m_{H_2}^2)) = 0$.

(m_{H_1}, m_{H_2}), we focus on the case of $m_{\eta^+} = m_{H_2}$ for simplicity. The operation of switching $H_1 \leftrightarrow H_2$ is to shift the mixing angle by $\alpha \to (\alpha - \frac{\pi}{4})$. The 1σ EWPT fit prefers the mass splitting $(m_{H_2} - m_{H_1}) > 0$ in a small range of $0.92 < \cos\alpha < 1.0$; i.e., $H_2(A_2)$ dominantly composed of $\eta_R(\eta_I)$ should be heavier. However, at the 3σ fit, $(m_{H_2} - m_{H_1})$ is permitted in either sign $(+/-)$ for $0 < \alpha < \frac{\pi}{2}$, with its magnitude decreasing with $\cos\alpha$. In the right plot, we show that assuming $m_{H_2} > m_{H_1}$, the $S - T$ bound requires $(m_{H_2} - m_{H_1}) \subset (30, 120)$ GeV at 1σ and $(m_{H_2} - m_{H_1}) < 150$ GeV at 3σ for $100 < m_{H_1} < 500$ GeV under the condition specified in the caption.

III. DARK MATTER

The relic density for a DM species X is determined by its energy density, $\propto m_X n_X(T_0)$ in the present Universe, where the number density n_X is governed by the Boltzmann equation during the decoupling phase plus the expansion effect afterwards. For a Dirac fermion DM stabilized by a $\mathbb{Z}_3$ symmetry, semiannihilation modes, in addition to annihilation, are expected to contribute. The Boltzmann equation can be recast into an evolution in terms of a yield by defining $Y_X = n_X/s$ with s as the entropy density and $x = M_X/T$ where the temperature is scaled by the DM mass. The redefined equation reads

$$\frac{dY_X}{dx} = -\frac{\lambda_A}{x^2}[Y_X^2 - Y_X^{eq2}] - \frac{1}{2}\frac{\lambda_S}{x^2}[Y_X^2 - Y_X Y_X^{eq}], \quad (3.1)$$

$$\lambda_i = \frac{s(x=1)}{H(x=1)}\langle \sigma v_{rel}\rangle_i, \qquad i = A, S,$$

$$s(x=1) = \frac{2\pi^2}{45}g_* M_X^3, \qquad H(x=1) = \sqrt{\frac{\pi^2}{90}g_*}\frac{M_X^2}{M_{pl}} \quad (3.2)$$

where A, S stand for annihilation and semiannihilation, $H(x=1)$ is the Hubble constant at $T = M_X$, g_* is the effective total number of relativistic degrees of freedom, and $M_{pl} = 1.22 \times 10^{19}$[GeV] is the Planck mass. The $\frac{1}{2}$ factor in the second term of Eq. (3.1) is due to the identical *initial* particles,[3] and $\langle \sigma v_{rel}\rangle$ is the thermal average of the velocity-weighted cross section, which represents the DM interaction rate. This equation can be analytically solved in

---

[3]For the semiannihilation, considering the evolution of the number density for one species X, we need to take into account the processes of $XX \to \bar{X}\nu_i$ and $\bar{X}\bar{X} \to X\bar{\nu}_i$, where the number of the species X is only depleted by 1 in the forward direction, which is the same as in the particle-antiparticle annihilation. Thus, the Boltzmann equation with only the semiannihilation mode should be $\frac{dn_X}{dt} + 3Hn_X = -\frac{1}{2}\langle \sigma v\rangle_{Semi}[n_X^2 - n_X n_X^{eq}]$. This is different from the DM annihilation of Majorana fermions, where the depletion number is 2, and it compensates the phase space factor $\frac{1}{2}$ from identical particles.

a proper approximation by matching the results from two regions at the freeze-out point. A brief review for this approach will be presented here in order to clarify the missing $1/2$ in some of the literature. We start by defining a quality $\Delta = Y_X - Y_X^{eq}$, so the original equation is transformed into

$$\frac{d\Delta}{dx} = -\frac{dY_X^{eq}}{x} - \frac{\lambda_A}{x^2}[\Delta^2 + 2\Delta Y_X^{eq}] - \frac{1}{2}\frac{\lambda_S}{x^2}[\Delta^2 + \Delta Y_X^{eq}] \quad (3.3)$$

where the Maxwell-Boltzmann distribution will be used for the yield in equilibrium so that $Y_X^{eq}(x) \propto x^{3/2}e^{-x}$. For $x \ll x_f$, we can obtain

$$\Delta = \frac{Y_X^{eq}}{\frac{\lambda_A}{x^2}(2Y_X^{eq} + \Delta) + \frac{\lambda_S}{2x^2}(Y_X^{eq} + \Delta)}, \quad (3.4)$$

and for $x \gg x_f$, the integration of the Boltzmann equation gives

$$Y_X(\infty) \simeq -\int_{x_f}^{\infty} dx \frac{\lambda_A + \frac{1}{2}\lambda_S}{x^2}. \quad (3.5)$$

Thus, the relic density at the present Universe is found as

$$\Omega h^2 = m_X s_0 Y_X(\infty)/\rho_c \approx 2\frac{1.07 \times 10^9 \text{ GeV}^{-1}}{\sqrt{g_*(x_f)}M_{pl}J(x_f)}, \quad (3.6)$$

$$J(x_f) = \int_{x_f}^{\infty} dx \frac{\langle \sigma v_{rel}\rangle_A + \frac{1}{2}\langle \sigma v_{rel}\rangle_S}{x^2}, \quad (3.7)$$

where Ωh^2 is rescaled by the critical density $\rho_c = 3H^2/8\pi G$. We multiply by a factor 2 for the relic density in order to count the contribution from the antiparticle $\bar{X}$ and set $g_*(x_f) \approx 100$ at the point of freeze-out. Here $\langle \sigma v\rangle_A$ is the thermal average for annihilation, while $\langle \sigma v\rangle_S$ is for semiannihilation. Then the freeze-out temperature x_f is determined by the boundary condition $\Delta(x_f) = cY_X^{eq}(x_f)$ with $c = \sqrt{2} - 1$ as

$$x_f \simeq \ln\left[0.038c(c+2)\langle \sigma v\rangle_A \frac{gM_X M_{pl}}{\sqrt{g_* x_f}}\right]$$

$$+ \ln\left[1 + \frac{c+1}{c+2}\frac{\langle \sigma v\rangle_S}{2\langle \sigma v\rangle_A}\right], \quad (3.8)$$

which is up to a factor of $1/2$ for the semiannihilation part as given by [6], and we set $g = 2$ for a fermion DM of 2 degrees of freedom without counting its antiparticle [33].

We can see that in order to estimate the relic density, one has to calculate the thermal average of the cross section times the relative velocity $\langle \sigma v_{rel}\rangle$. Generally, the thermal average is approximated by an expansion on the order of x^{-n} ($\langle v^2\rangle \sim \frac{6}{x}$ in the nonrelativistic limit). However, in our
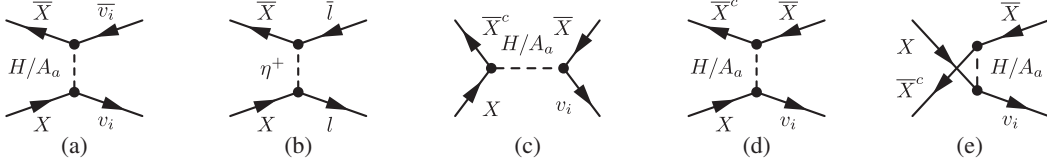
FIG. 5.   Feynman diagrams for the annihilation (a, b) and semiannihilation processes (c)–(e), where the mediating scalar fields are H_a or A_a, with $a = 1, 2$.

case, the dominant DM cross section proceeds through an s-channel with one very narrow resonance $\Gamma_M/M_X \ll v_{\rm rel}$ and one wider resonance $\Gamma_M/M_X \sim v_{\rm rel}$. In addition, for an s-channel interaction mediated by a scalar, the s-wave is vanishing for the velocity averaged cross section; thus the expansion in terms of $v_{\rm rel}^2$ is complicated for two resonances interfering with each other. We prefer to use the integration approach to evaluate $\langle \sigma v_{\rm rel} \rangle$, which is given by [34,35]

$$\langle \sigma v_{\rm rel} \rangle_A = \sum_{i=1}^{2} \frac{\int_{4M_X^2}^{\infty} ds \sigma_{XX}^i (s - 4M_X^2)\sqrt{s} K_1(\frac{\sqrt{s}}{M_X}x)}{8M_X^5 x^{-1} K_2(x)^2}, \quad (3.9)$$

$$\langle \sigma v_{\rm rel} \rangle_S = \frac{\int_{4M_X^2}^{\infty} ds \sigma_{XX}^3 (s - 4M_X^2)\sqrt{s} K_1(\frac{\sqrt{s}}{M_X}x)}{8M_X^5 x^{-1} K_2(x)^2}, \quad (3.10)$$

where $s = (k_1 + k_2)^2$ is a Mandelstam variable and $K_{1,2}$ are the modified Bessel functions of order 1 and 2, respectively:

$$\sigma_{XX}^i = \frac{|\mathbf{k}_1|}{32\pi^2 s \sqrt{s - 4M_X^2}} \int d\Omega |\bar{\mathcal{M}}_i|^2, \quad i = 1, 2, 3;$$

with $|\mathbf{k}_1| = \sqrt{\frac{s}{4} - m_{l/\nu}^2}$ $i = 1, 2;$ $|\mathbf{k}_1| = \frac{s - M_X^2}{2\sqrt{s}} i = 3.$

$$(3.11)$$

Here σ_{XX}^i is the cross section of the $2 \to 2$ process (denoting $\mathbf{k}_1$ as the 3-momentum of the first outgoing particle) and with the amplitude squared $|\bar{\mathcal{M}}_{1,2}|^2$ corresponding to $X\bar{X} \to \nu_i \bar{\nu}_j$ and $X\bar{X} \to \ell_i \bar{\ell}_j$ in Figs. 5(a) and 5(b) and the third $|\bar{\mathcal{M}}_3|^2$ standing for $XX \to \bar{X}\nu_i$, i.e., the semiannihilation as depicted in Figs. 5(c)–5(e).

We derive the analytic expression for each amplitude squared present in Eq. (3.11). Let us consider the case where only the lightest flavor of χ_i is the DM candidate. By defining $X = \chi_1$ and assuming $y_\chi^L = y_\chi^R$, the DM-scalar interaction in this model is written as

$$-\mathcal{L} = \frac{y_{\eta_{i1}}}{\sqrt{2}} \bar{\nu}_i P_R X (s_\alpha H_1 + c_\alpha H_2) - i \frac{y_{\eta_{i1}}}{\sqrt{2}} \bar{\nu}_i P_R X (s_\alpha A_1 + c_\alpha A_2) - y_{\eta_{i1}} \bar{\ell}_i P_R X \eta^-$$

$$+ \frac{y_{\chi_{11}}}{\sqrt{2}} \bar{X}^C X (c_\alpha H_1 - s_\alpha H_2) + i \frac{y_{\chi_{11}}}{\sqrt{2}} \bar{X}^C X (c_\alpha A_1 - s_\alpha A_2) + {\rm H.c.} \quad (3.12)$$

For the annihilation processes, $|\bar{\mathcal{M}}_{1,2}|$ are the usual amplitudes squared with the spin averaged for the initial states and summed for the final states. However, a special treatment is needed for $|\bar{\mathcal{M}}_3|$ because of the identical incoming particles. As illustrated in Figs. 5(c)–5(e), the semiannihilation proceeds in S, T, and U channels after counting the momentum exchange for the identical *initial* particles. In particular, there is a symmetry factor 2 for the s-channel amplitude.[4] Combining all channels, we can arrive at the following analytic expressions:

$$|\bar{\mathcal{M}}_1|^2 = \sum_{i,j=1}^{3} |y_{\eta_{i1}} y_{\eta_{1j}}^\dagger|^2 \left| \frac{s_\alpha^2}{M_X^2 - m_{H_1}^2 - 2p_1 \cdot k_1} + \frac{c_\alpha^2}{M_X^2 - m_{H_2}^2 - 2p_1 \cdot k_1} \right|^2 (p_1 \cdot k_1)(p_2 \cdot k_2), \quad (3.13)$$

$$|\bar{\mathcal{M}}_2|^2 = \sum_{i,j=1}^{3} \left| \frac{y_{\eta_{i1}} y_{\eta_{1j}}^\dagger}{M_X^2 - m_{\eta^\pm}^2 - 2p_1 \cdot k_1} \right|^2 (p_1 \cdot k_1)(p_2 \cdot k_2), \quad (3.14)$$

---

[4]We need to consider the momentum exchange for the identical *initial* particles due to the phase space integration in the thermal average. For semiannihilation $X(p_1)X(p_2) + X(p_2)X(p_1) \to \bar{X}(k_1)v_i(k_2)$, the s-channel amplitude is proportional to $[\bar{u}^c(p_1)u(p_2) - \bar{u}^c(p_2)u(p_1)][\bar{v}(k_1)u(k_2)] = 2[\bar{v}(p_1)u(p_2)][\bar{v}(k_1)u(k_2)]$, where we use the identities $u^c = C\bar{u}^T = v$ and $\bar{v}(p_2)u(p_1) = u^T(p_1)C^{-1}C\bar{v}^T(p_2) = -\bar{v}(p_1)u(p_2)$, with $C = i\gamma^0\gamma^2$ being the charge conjugate operator. This is similar to the identical scalar case $\phi\phi \to H_a$; the symmetry factor is normally encoded in the vertex.

$$\begin{aligned}
|\bar{\mathcal{M}}_3|^2 = (s_\alpha c_\alpha)^2 \sum_{i=1}^{3} |y_{\chi_{11}} y_{\eta_{i1}}|^2 &\Bigg[8 \Bigg| \sum_{a=1}^{2} (-1)^{a+1} S_{\text{inv}}^a \Bigg|^2 (p_1 \cdot p_2 - M_X^2)(k_1 \cdot k_2) \\
&+ 2 \Bigg| \sum_{a=1}^{2} (-1)^{a+1} T_{\text{inv}}^a \Bigg|^2 (p_1 \cdot k_1 + M_X^2)(p_2 \cdot k_2) + 2 \Bigg| \sum_{a=1}^{2} (-1)^{a+1} U_{\text{inv}}^a \Bigg|^2 (p_2 \cdot k_1 + M_X^2) p_1 \cdot k_2 \\
&+ 2 \sum_{a=1}^{2} (-1)^{a+1} S_{\text{inv}}^{\text{Re},a} \sum_{a=1}^{2} (-1)^{a+1} T_{\text{inv}}^a [(p_1 \cdot p_2)(k_1 \cdot k_2) - (p_1 \cdot k_2)(p_2 \cdot k_1) + (p_1 \cdot k_1)(p_2 \cdot k_2) \\
&+ M_X^2(-p_1 \cdot k_2 + p_2 \cdot k_2 - k_1 \cdot k_2)] + 2 \sum_{a=1}^{2} (-1)^{a+1} S_{\text{inv}}^{\text{Re},a} \sum_{a=1}^{2} (-1)^{a+1} U_{\text{inv}}^a [(p_1 \cdot p_2)(k_1 \cdot k_2) \\
&- (p_1 \cdot k_1)(p_2 \cdot k_2) + (p_1 \cdot k_2)(p_2 \cdot k_1) + M_X^2(-p_2 \cdot k_2 + p_1 \cdot k_2 - k_1 \cdot k_2)] \\
&- \sum_{a=1}^{2} (-1)^{a+1} T_{\text{inv}}^a \sum_{a=1}^{2} (-1)^{a+1} U_{\text{inv}}^a [(p_1 \cdot k_1)(p_2 \cdot k_2) - (p_1 \cdot p_2)(k_1 \cdot k_2) + (p_1 \cdot k_2)(p_2 \cdot k_1) \\
&+ M_X^2(k_1 \cdot k_2 + p_1 \cdot k_2 + p_2 \cdot k_2)] \Bigg].
\end{aligned} \tag{3.15}$$

In the $\mathcal{M}_3$ amplitude of semiannihilation, we define $S_{\text{inv}}^a = 1/(s - m_a^2 + i m_a \Gamma_a)$, $T_{\text{inv}}^a = 1/(2M_X^2 - m_a^2 - 2p_1 \cdot k_1)$, $U_{\text{inv}}^a = 1/(M_X^2 - m_a^2 - 2p_1 \cdot k_2)$, and the index $a = 1, 2$ corresponds to $H_1(A_1)$, $H_2(A_2)$, respectively. The inner products are given in Appendix C.

For the s-channel amplitude, the widths of inert scalars $H_{1,2}(A_{1,2})$ enter into the Breit-Wigner propagator S_{inv}^a, whose magnitude near two on-shell poles $m_{H_1} = 2M_X$ or $m_{H_2} = 2M_X$ is determined by the Γ_{H_1} or Γ_{H_2}. Under this consideration, we will only be interested in the parameter region $m_{H_1} < m_{H_2} < \min(m_{E_i'}, m_{\chi_2}, m_{\chi_3})$ to ensure a narrow resonance. Therefore, the decay widths of $\Gamma_{H_1} (= \Gamma_{A_1})$ and $\Gamma_{H_2} (= \Gamma_{A_2})$ are formulated as

$$\Gamma_{H_1} = \theta(m_{H_1} - 2M_X)\Gamma(H_1 \to XX + \bar{X}\bar{X}) + \theta(m_{H_1} - M_X)\Gamma(H_1 \to X\bar{v}_i + \bar{X}v_i)$$

$$\Gamma(H_1 \to XX + \bar{X}\bar{X}) = |y_{\chi_{11}}|^2 c_\alpha^2 \frac{(m_{H_1}^2 - 4M_X^2)^{3/2}}{4\pi m_{H_1}^2}$$

$$\Gamma(H_1 \to X\bar{v}_i + \bar{X}v_i) = \sum_{i}^{3} |y_{\eta_{i1}} y_{\eta_{1i}}^\dagger| s_\alpha^2 \frac{(m_{H_1}^2 - M_X^2)^2}{16\pi m_{H_1}^3}, \tag{3.16}$$

and for H_2, one more decay channel $H_2 \to H_1 h_0$, with a coupling vertex of $\frac{1}{2}\lambda_0 v_\varphi (c_\alpha^2 - s_\alpha^2) = s_\alpha c_\alpha (c_\alpha^2 - s_\alpha^2)(m_{H_1}^2 - m_{H_2}^2)/v_H$ and h_0 being the SM Higgs boson, will be open if it is permitted by kinematics,

$$\begin{aligned}
\Gamma_{H_2} = &\theta(m_{H_2} - 2M_X)\Gamma(H_2 \to XX + \bar{X}\bar{X}) + \theta(m_{H_2} - M_X)\Gamma(H_2 \to X\bar{v}_i + \bar{X}v_i) \\
&+ \theta(m_{H_2} - M_{H_1} - m_{h_0})\Gamma(H_2 \to H_1 h_0)
\end{aligned}$$

$$\Gamma(H_2 \to XX + \bar{X}\bar{X}) = |y_{\chi_{11}}|^2 s_\alpha^2 \frac{(m_{H_2}^2 - 4M_X^2)^{3/2}}{4\pi m_{H_2}^2}$$

$$\Gamma(H_2 \to X\bar{v}_i + \bar{X}v_i) = \sum_{i}^{3} |y_{\eta_{i1}} y_{\eta_{1i}}^\dagger| c_\alpha^2 \frac{(m_{H_2}^2 - M_X^2)^2}{16\pi m_{H_2}^3}$$

$$\Gamma(H_2 \to H_1 h_0) = s_\alpha^2 c_\alpha^2 (c_\alpha^2 - s_\alpha^2)^2 \frac{(m_{H_2}^2 - m_{H_1}^2)^2}{16\pi v_H^2 m_{H_2}^3}$$

$$\times [(m_{H_2}^2 - (m_{H_1} + m_{h_0})^2)(m_{H_2}^2 - (m_{H_1} - m_{h_0})^2)]^{1/2} \tag{3.17}$$

where the step function is defined as $\theta(x) = 1$ only for $x > 0$ and otherwise it is zero.

A. Relic density analysis

In this section, we show that the numerical analysis satisfies all the constraints discussed in Sec. II. We find that after imposing the LFV bounds and neutrino oscillation data, one DM-neutrino-scalar coupling $y_{\eta_{il}}$ populates in the range of $(10^{-3}, 1.0)$, so the annihilation process in this model cannot account for a correct relic density. However, a large enhancement for $\langle \sigma v \rangle$ could be achieved if the semiannihilation proceeds through an s-channel and in the vicinity of one narrow-width resonance. Since Eq. (3.15) indicates that two resonances of complex scalars are deconstructive, the condition $100 < (m_{H_2} - m_{H_1}) < 150$ GeV is imposed in the analysis, with the upper limit from the 3σ EWPT fit at $\cos \alpha = \frac{1}{\sqrt{2}}$. Thus, for a given DM mass, only one resonance can effectively be on shell. On the other hand, we require $m_{H'_1} \simeq m_{H'_2}$, i.e., quasidegenerate, in order to satisfy the neutrino oscillation data. This condition can be easily fulfilled if we make the mixing term $\lambda'_0 H^\dagger \eta' s'^* \varphi^*$ tiny. In order to simplify the analysis, we adopt several assumptions:

$$m_{\eta^\pm} = m_{H_2}, \qquad y'_{\eta'} = y_{\eta'}, \qquad y'_{s'} = y_{s'},$$
$$s_\alpha = s_{\alpha'} = c_\alpha = c_{\alpha'} = \frac{1}{\sqrt{2}}. \qquad (3.18)$$

We set $m_{\eta^\pm} = m_{H_2}$, which is consistent with the EWPT bound, as shown in Fig. 4, and $y'_{\eta'}, y'_{s'}$ are taken to be diagonal matrices. Under these assumptions, a numerical scan is conducted for the parameter space by imposing the relevant neutrino and LFV bounds and limiting the relic density to be $0.117 < \Omega h^2 < 0.123$. We explore the two on-shell scenarios in two overlapping DM mass regions with $m_{H_1} = 2M_X$ for $80 < M_X < 350$ GeV and $m_{H_2} = 2M_X$ for $200 < M_X < 400$ GeV. Furthermore, in order to work well

under the Breit-Wigner narrow-width prescription, we remove the points with $\max\left(\frac{\Gamma_{H_1}}{m_{H_1}}, \frac{\Gamma_{H_2}}{m_{H_2}}\right) > 0.2$. For the latter case of $m_{H_2} = 2M_X$, we impose a smaller splitting $(m_{H_2} - m_{H_1}) \simeq (115, 125)$ GeV; thus $m_{H_1} \gg m_X$. This condition will ensure $\Gamma_{H_1} \ll m_{H_1}$ and avoid coannihilation from scalars. From the left plot in Fig. 6, we can see that the observed relic density dominantly comes from the semiannihilation. At the time of freeze-out, $x_f \approx 21.0$ [calculated by Eq. (3.8)], the thermal average of the cross section is within the range of 5.98×10^{-10} GeV$^{-2} \lesssim \langle \sigma v_{\text{Semi}} \rangle \lesssim 8.83 \times 10^{-10}$ GeV^{-2}, where the larger value normally corresponds to a larger DM mass. In the right plot, we show the allowed region in the $(M_X, y_{\chi_{11}})$ plane with other parameters randomly scanned. The plot demonstrates that a small DM mass $M_X < 200$ GeV is more sensitive to the lighter $H_1 + iA_1$ resonance and permits a DM Yukawa coupling $y_{\chi_{11}} \gtrsim 0.1$. However, for $M_X > 200$ GeV, our fitting analysis indicates a larger DM coupling $y_{\chi_{11}} \gtrsim 0.5$, which is close to the perturbative limit $\sqrt{4\pi}$ regardless of the lighter or heavier resonance scenario.

Figure 7 presents the mass ranges for $M_{E'}(= M_{N'})$ and M_N, which enter into the numerator of neutrino mass form factors as well as values of $|\Delta a_\mu|$ versus M_X. The typical value for the lightest vectorlike fermions L'_i lies in the range 0.5–2.5 TeV, but the degeneracy results in no effect on EWPT. Also, this mass range of $M_{E'}$ is not sensitive to the LHC bound for charged lepton pairs plus missing transverse energy [36]. While after enforcing all the bounds, the maximum value for $|\Delta a_\mu|$ is of order $\lesssim 10^{-14}$, and even lower for most benchmark points, it is negligible compared with the 3.6σ deviation of order 10^{-9} as measured by the experiment. Thus, this model cannot simultaneously account for the large discrepancy in the muon $g - 2$.
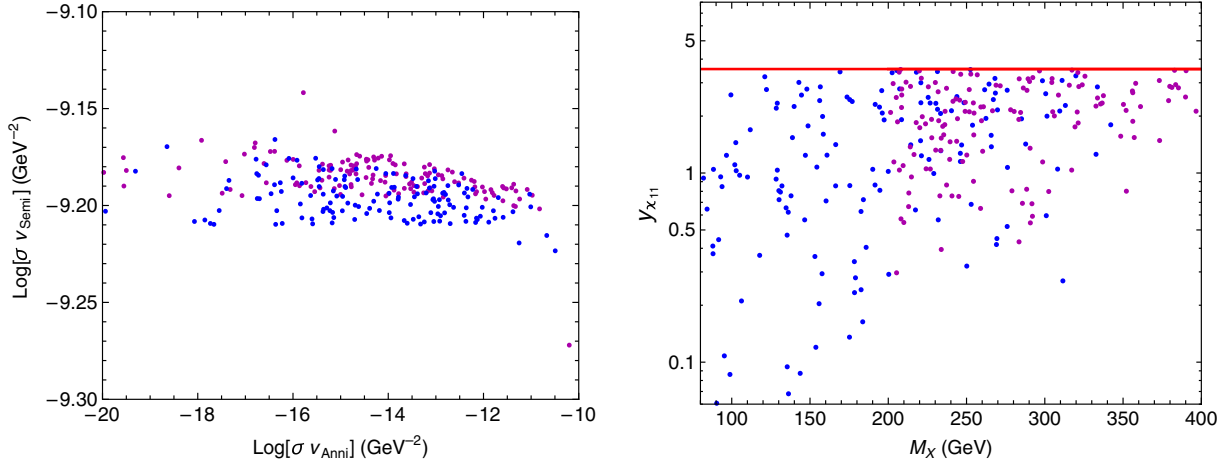

FIG. 6.   The left plot shows the thermal average $\langle \sigma v_{\text{Anni}} \rangle$ for annihilation versus the thermal average $\langle \sigma v_{\text{Semi}} \rangle$ for semiannihilation at the freeze-out temperature. The right plot illustrates the allowed region in the plane of $(M_X, y_{\chi_{11}})$, with the red line signaling the perturbation limit $y_{\chi_{11}} < \sqrt{4\pi}$. The blue points represent the scenario of $m_{H_1} = 2M_X$ (lighter resonance), and the magenta points stand for the scenario of $m_{H_2} = 2M_X$ (heavier resonance). All points satisfy the LFV bounds, neutrino data, and Planck satellite measurement $0.117 < \Omega h^2 < 0.123$ at the 3σ confidence level.
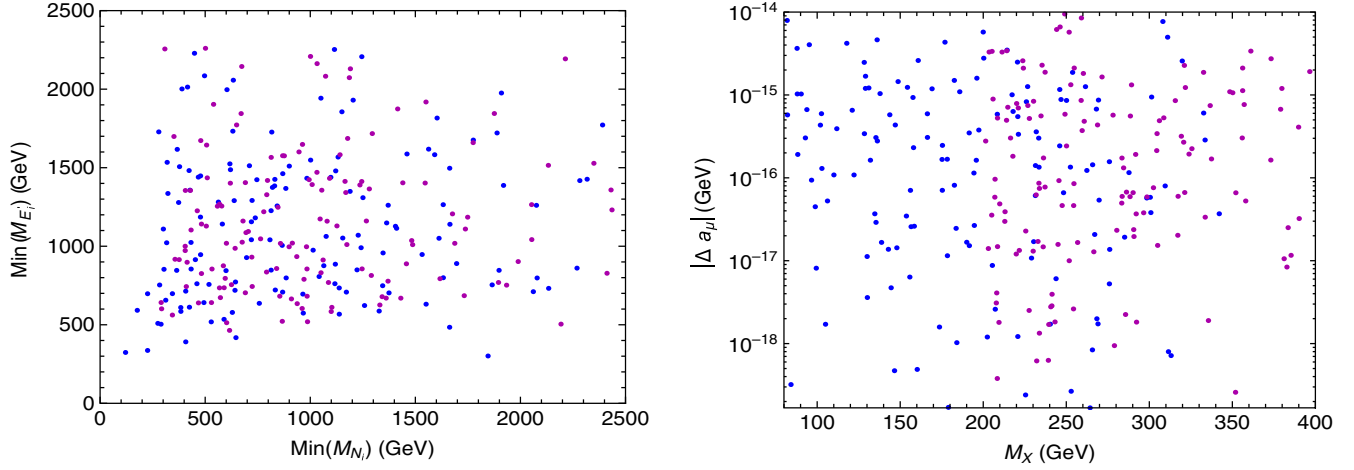
FIG. 7.   The left plot shows the lightest mass in $M_{E_i'}, i = 1, 2, 3$ versus the lightest mass in $M_{N_i}, i = 1, 2, 3$. The right plot illustrates the correlation of $|\Delta a_\mu|$ to the DM mass M_X. The blue points represent the scenario of $m_{H_1} = 2M_X$, and the magenta points stand for the scenario of $m_{H_2} = 2M_X$. All points satisfy the LFV bounds, neutrino data, and Planck satellite measurement $0.117 < \Omega h^2 < 0.123$ at the 3σ confidence level.

Direct detection.—In our case, there are no direction interactions between $H_{1,2}/A_{1,2}$ and the quarks at the tree level; therefore, the constraints of direct detection searches should be satisfied without difficulty.

IV. CONCLUSIONS AND DISCUSSIONS

We have constructed a neutrino mass model based on hidden local $U(1)_H$ symmetry, which gives rise to a Dirac fermion type of dark matter. The neutrino masses are generated at the two-loop level due to the symmetry and particle content. Furthermore, because the form factor of the neutrino mass is proportional to the mass squared differences of inert scalars, we require one set of inert scalars to be quasidegenerate so that a sub-eV scale neutrino mass can be achieved without large fine-tuning for the Yukawa couplings. As a variation to this model, we illustrate that the heavy Z' associated with the $U(1)$ will not impact the DM annihilation because its mixing with the SM Z boson is induced by a complex triplet field Δ, whose VEV is severely constrained by the ρ parameter. Particularly, the presence of inert scalars (η, s) gives rise to notable S and T deviations. Note that the impact of singlet s on oblique parameters is via the mixing with doublet η. The 3σ EWPT fit prefers the mass splitting of $|m_{H_2} - m_{H_1}| \lesssim 150$ GeV, provided $\cos\alpha = \frac{1}{\sqrt{2}}$ and $m_\eta^+ = m_{H_2}$.

Our DM is the lightest neutral particle stabilized by a discrete $\mathbb{Z}_3$ parity, which is a residual symmetry of $U(1)_H$

after spontaneous symmetry breaking. Therefore, in addition to the standard DM annihilation process, DM semiannihilation is induced in this model. After imposing the LFV bounds and neutrino oscillation data and assuming no specific flavor structure in Yukawa couplings, we find that the s-channel semiannihilation plays an important role to determine the observed relic density with a DM mass of $\mathcal{O}(100)$ GeV. Our analysis demonstrates that the lighter and heavier resonances can contribute significantly when either one is actually put on shell and the allowed DM-scalar Yukawa coupling is in the range of $(0.1-\sqrt{4\pi})$, depending on the DM mass region.

APPENDIX A: LOOP FUNCTIONS FOR NEUTRINO MASS

The neutrino mass in this radiative seesaw model is generated by the two-loop Feynman diagrams in Fig. 2. It is convenient to decompose the mass matrix as $(m_\nu)_{ij} = m_{\nu_{ij}}^{(I)} + m_{\nu_{ij}}^{(II)} + [m_{\nu_{ij}}^{(I)}]^T + [m_{\nu_{ij}}^{(II)}]^T$, with $m_{\nu_{ij}}^{(I)}$ and $m_{\nu_{ij}}^{(II)}$ calculated as

$$m_\nu^{(I)} = y_{\eta_{ia}} y_{s'_{ap}}^T y_{\eta'_{pb}} y_{S_{bj}}^T s_\alpha c_\alpha s'_\alpha c'_\alpha \int \frac{d^4 k_1}{(2\pi)^4} \int \frac{d^4 k_2}{(2\pi)^4} \frac{-M_{N_\rho} k_2^2}{(k_1^2 - M_{N_\rho}^2)(k_2^2 - M_{X_a}^2)(k_2^2 - M_{N_b'}^2)}$$

$$\times \left(\frac{1}{k_2^2 - m_{H_1}^2} - \frac{1}{k_2^2 - m_{H_2}^2} \right) \left(\frac{1}{(k_1 - k_2)^2 - m_{H_1'}^2} - \frac{1}{k_2^2 - m_{H_2'}^2} \right), \tag{A1}$$

$$m_\nu^{(II)} = y_{\eta_{ia}} y_{s'_{a\rho}}'^T y_{\eta'_{\rho b}}' y_{S_{bj}}^T s_\alpha c_\alpha s'_\alpha c'_\alpha \int \frac{d^4 k_1}{(2\pi)^4} \int \frac{d^4 k_2}{(2\pi)^4} \frac{M_{\chi_a} M_{N_\rho} M_{N'_b}}{(k_1^2 - M_{N_\rho}^2)(k_2^2 - M_{\chi_a}^2)(k_2^2 - M_{N'_b}^2)}$$

$$\times \left(\frac{1}{k_2^2 - m_{H_1}^2} - \frac{1}{k_2^2 - m_{H_2}^2} \right) \left(\frac{1}{(k_1 - k_2)^2 - m_{H'_1}^2} - \frac{1}{k_2^2 - m_{H'_2}^2} \right). \tag{A2}$$

For clarity, we can redefine $m_{\nu_{ij}}^{(I/II)} = \frac{1}{(4\pi)^4} y_{\eta_{ia}} F_{I/II}(H_{1,2}, H'_{1,2})_{ab} y_{bj}^T$ by extracting out a loop factor and Yukawa couplings in the outer loop of Feynman diagrams. After imposing the Feynman parametrization, the two-loop functions $F_{I/II}(H_{1,2}, H'_{1,2})$ are given by

$$F_I(H_{1,2}, H'_{1,2})_{ab} = 2 y_{s'_{a\rho}}^T M_{N_\rho} y_{\eta'_{\rho b}}' (m_{H_1}^2 - m_{H_2}^2)(m'^2_{H_1} - m'^2_{H_2}) s_\alpha c_\alpha s_{\alpha'} c_{\alpha'}$$

$$\times \int \frac{[da]_3 [d\alpha]_5 a(b+c)}{[\alpha(a M_{N_\rho}^2 + b m_{H'_1}^2 + c m_{H'_2}^2) + a(b+c)(\beta M_{\chi_a}^2 + \gamma M_{N'_b}^2 + \rho m_{H_1}^2 + \sigma m_{H_2}^2)]^2}, \tag{A3}$$

$$F_{II}(H_{1,2}, H'_{1,2})_{ab} = 2 M_{\chi_a} y_{s'_{a\rho}}'^T M_{N_\rho} y_{\eta'_{\rho b}}' M_{N'_b} (m_{H_1}^2 - m_{H_2}^2)(m'^2_{H_1} - m'^2_{H_2}) s_\alpha c_\alpha s_{\alpha'} c_{\alpha'}$$

$$\times \int \frac{[da]_3 [d\alpha]_5 a^2(b+c)^2}{[\alpha(a M_{N_\rho}^2 + b m_{H'_1}^2 + c m_{H'_2}^2) + a(b+c)(\beta M_{\chi_a}^2 + \gamma M_{N'_b}^2 + \rho m_{H_1}^2 + \sigma m_{H_2}^2)]^3}, \tag{A4}$$

where we use the definitions $[da]_3 \equiv \int_0^1 db \int_0^{1-b} dc$ with $a = 1 - b - c$, and $[d\alpha]_5 \equiv \int_0^1 d\alpha \int_0^{1-\alpha} d\beta \int_0^{1-\alpha-\beta} d\gamma \times \int_0^{1-\alpha-\beta-\gamma} d\rho$ with $\sigma = 1 - \alpha - \beta - \gamma - \rho$. Note that these form factors are finite and will be numerically evaluated.

APPENDIX B: *T* PARAMETER FROM MIXING INERT SCALARS

Since the longitude modes of W, Z gauge bosons are $\partial_\mu G^{\pm,0}$, the T parameter is easily calculated from the wave-function renormalization of Goldstone bosons. We show that the two approaches match with each other. The relevant terms from the scalar potential are

$$\mathcal{V} \supset -\mu_H^2 H^\dagger H + \lambda_H (H^\dagger H)^2 + \lambda_{H\eta} (H^\dagger H)(\eta^\dagger \eta)$$

$$+ \lambda'_{H\eta} (H^\dagger \eta)(\eta^\dagger H) + \lambda_{\varphi\eta} (\varphi^\dagger H)(\eta^\dagger \eta)$$

$$+ \lambda_{Hs} (H^\dagger H)(s^* s) + \lambda_{\varphi s} (\varphi^\dagger \varphi)(s^* s)$$

$$+ (\lambda_0 H^\dagger \eta s^* \varphi + \text{H.c.}) + \mu_\eta^2 \eta^\dagger \eta + \mu_s^2 s^* s. \tag{B1}$$

Due to the $\mathbb{Z}^3$ parity, there is no mass splitting among the imaginary and real parts of inert neutral scalars. The masses can be read off from Eq. (B1):

$$m_{\eta^+}^2 = \mu_\eta^2 + \frac{1}{2}(\lambda_{H\eta} v_H^2 + \lambda_{\varphi\eta} v_\varphi^2), \tag{B2}$$

$$\frac{1}{2} \begin{pmatrix} s_{R/I} \\ \eta_{R/I} \end{pmatrix}^T \begin{bmatrix} m_{s_R}^2 & \frac{1}{2}\lambda_0 v_H v_\varphi \\ \frac{1}{2}\lambda_0 v_H v_\varphi & m_{\eta_R}^2 \end{bmatrix} \begin{pmatrix} s_{R/I} \\ \eta_{R/I} \end{pmatrix}, \tag{B3}$$

with the diagonal parts

$$m_{s_R}^2 = \mu_s^2 + \frac{1}{2}(\lambda_{Hs} v_H^2 + \lambda_{\varphi s} v_\varphi^2),$$

$$m_{\eta_R}^2 = \mu_\eta^2 + \frac{1}{2}(\lambda_{H\eta} v_H^2 + \lambda_{\varphi\eta} v_\varphi^2 + \lambda'_{H\eta} v_H^2). \tag{B4}$$

The following identities will hold for the mass eigenstates and rotating angle:

$$m_{s_R}^2 = m_{H_1}^2 \cos^2 \alpha + m_{H_2}^2 \sin^2 \alpha$$

$$m_{\eta_R}^2 = m_{H_1}^2 \sin^2 \alpha + m_{H_2}^2 \cos^2 \alpha$$

$$\sin 2\alpha = \frac{\lambda_0 v_H v_\varphi}{m_{H_1}^2 - m_{H_2}^2}. \tag{B5}$$

Since $\delta\rho = \delta Z_{G^+} - \delta Z_{G^0}$, the two-point self-energy diagrams in Fig. 8 give us

$$\hat{\alpha}\Delta T = 2 \left(\lambda'_{H\eta} \frac{v_H}{2} \sin \alpha + \lambda_0 \frac{v_\varphi}{2} \cos \alpha \right)^2 f(m_{H_1}, m_{\eta^+})$$

$$+ 2 \left(\lambda'_{H\eta} \frac{v_H}{2} \cos \alpha - \lambda_0 \frac{v_\varphi}{2} \sin \alpha \right)^2 f(m_{H_2}, m_{\eta^+})$$

$$- \frac{1}{2} \lambda_0^2 v_\varphi^2 f(m_{H_1}, m_{H_2}) \tag{B6}$$

with the function $f(m_1, m_2) = -i \frac{d\Pi(p^2)}{dp^2} \big|_{p^2=0}$, and $\hat{\alpha} = \frac{e^2}{4\pi}$. The $\Pi(p^2)$ is defined as

$$\Pi(p^2) = \int \frac{d^4 k}{(2\pi)^4} \frac{1}{(k^2 - m_1^2)((k+p)^2 - m_2^2)}$$

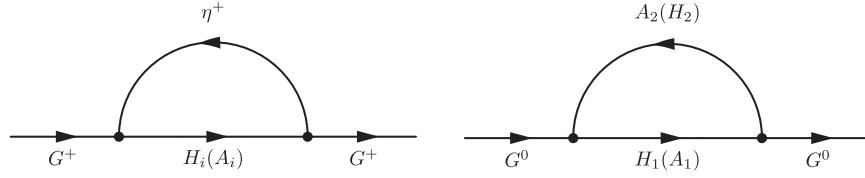$$= \int \frac{d^4 k}{(2\pi)^4} \int_0^1 dx \frac{1}{(k^2 - \Delta)^2} \tag{B7}$$

FIG. 8.   Self-energy diagrams for wave-function renormalization.

with $\Delta = -p^2(1-x)x + xm_1^2 + (1-x)m_2^2$. Thus, we can obtain the analytic formula

$$f(m_1, m_2) = \frac{1}{16\pi^2} \frac{m_1^4 - m_2^4 + 2m_1^2 m_2^2 \log(\frac{m_2^2}{m_1^2})}{2(m_1^2 - m_2^2)^3}. \quad \text{(B8)}$$

Using Eqs. (B2), (B4), and (B5), the coefficients in Eq. (B6) are related as

$$\left(\lambda'_{H\eta} \frac{v_H}{2}\sin\alpha + \lambda_0 \frac{v_\varphi}{2}\cos\alpha\right)^2 = \frac{(m_{H_1}^2 - m_{\eta^+}^2)^2}{v_H^2}\sin^2\alpha$$

$$\left(\lambda'_{H\eta} \frac{v_H}{2}\cos\alpha - \lambda_0 \frac{v_\varphi}{2}\sin\alpha\right)^2 = \frac{(m_{H_2}^2 - m_{\eta^+}^2)^2}{v_H^2}\cos^2\alpha$$

$$\lambda_0^2 v_\varphi^2 = \frac{4(m_{H_1}^2 - m_{H_2}^2)^2}{v_H^2}$$

$$\times \sin\alpha^2 \cos^2\alpha. \quad \text{(B9)}$$

Then, after substituting those identities back into Eq. (B6), we obtain the ΔT expression in Eq. (2.28).

APPENDIX C: INNER PRODUCTS FOR THE AMPLITUDES

The inner products of incoming and outgoing momenta are:

$$pk = \sqrt{((s - m_1^2 - m_2^2)^2 - 4m_1^2 m_2^2)((s - n_1^2 - n_2^2)^2 - 4n_1^2 n_2^2)},$$

$$p_1 \cdot k_1 = \frac{1}{4s}(|(s + m_1^2 - m_2^2)(s + n_1^2 - n_2^2)| - pk\cos\theta),$$

$$p_1 \cdot k_2 = \frac{1}{4s}(|(s + m_1^2 - m_2^2)(s + n_2^2 - n_1^2)| + pk\cos\theta),$$

$$p_2 \cdot k_1 = \frac{1}{4s}(|(s + m_2^2 - m_1^2)(s + n_1^2 - n_2^2)| + pk\cos\theta),$$

$$p_2 \cdot k_2 = \frac{1}{4s}(|(s + m_2^2 - m_1^2)(s + n_2^2 - n_1^2)| - pk\cos\theta),$$

$$\text{(C1)}$$

where $s \equiv (p_1 + p_2)^2$ is the Mandelstam variable, $m_{1,2}(p_{1,2})$ are the initial state masses (momenta), and $n_{1,2}(k_{1,2})$ are the final state masses (momenta).

[1] N. Aghanim *et al.* (Planck Collaboration), arXiv:1807.06209.
[2] E. Ma, Phys. Rev. D **73**, 077301 (2006).
[3] B. W. Lee and S. Weinberg, Phys. Rev. Lett. **39**, 165 (1977).
[4] T. Hambye, J. High Energy Phys. 01 (2009) 028.
[5] T. Hambye and M. H. G. Tytgat, Phys. Lett. B **683**, 39 (2010).
[6] F. D'Eramo and J. Thaler, J. High Energy Phys. 06 (2010) 109.
[7] G. Belanger, K. Kannike, A. Pukhov, and M. Raidal, J. Cosmol. Astropart. Phys. 04 (**2012**) 010.
[8] A. Zee, Nucl. Phys. **B264**, 99 (1986); K. S. Babu, Phys. Lett. B **203**, 132 (1988).
[9] K. S. Babu and C. Macesanu, Phys. Rev. D **67**, 073010 (2003).
[10] E. Ma, Phys. Lett. B **662**, 49 (2008).
[11] Y. Kajiyama, H. Okada, and K. Yagyu, Nucl. Phys. **B874**, 198 (2013).
[12] Y. Kajiyama, H. Okada, and T. Toma, Phys. Rev. D **88**, 015029 (2013).
[13] M. Aoki, J. Kubo, and H. Takano, Phys. Rev. D **87**, 116001 (2013).
[14] P. Langacker, Rev. Mod. Phys. **81**, 1199 (2009).
[15] E. J. Chun and J. C. Park, J. Cosmol. Astropart. Phys. 02 (2009) 026.
[16] P. Ko and T. Nomura, Phys. Rev. D **94**, 115015 (2016).
[17] T. Nomura, H. Okada, and P. Wu, J. Cosmol. Astropart. Phys. 05 (2018) 053.
[18] E. Ma, I. Picek, and B. Radovcic, Phys. Lett. B **726**, 744 (2013).
[19] E. Ma, N. Pollard, R. Srivastava, and M. Zakeri, Phys. Lett. B **750**, 135 (2015).
[20] P. Ko and Y. Tang, J. Cosmol. Astropart. Phys. 01 (2015) 023.
[21] C. Bonilla, R. M. Fonseca, and J. W. F. Valle, Phys. Rev. D **92**, 075028 (2015).
[22] R. Primulando, J. Julio, and P. Uttayarat, J. High Energy Phys. 08 (2019) 024.
[23] Z. Maki, M. Nakagawa, and S. Sakata, Prog. Theor. Phys. **28**, 870 (1962).

[24] M. Tanabashi *et al.* (Particle Data Group), Phys. Rev. D **98,** 030001 (2018).

[25] H. Okada and Y. Orikasa, Phys. Rev. D **94,** 055002 (2016).

[26] A. M. Baldini *et al.* (MEG Collaboration), Eur. Phys. J. C **76,** 434 (2016).

[27] B. Aubert *et al.* (*BABAR* Collaboration), Phys. Rev. Lett. **104,** 021802 (2010).

[28] F. Renga (MEG Collaboration), Hyperfine Interact. **239**, 58 (2018).

[29] M. E. Peskin and T. Takeuchi, Phys. Rev. D **46**, 381 (1992).

[30] H. E. Haber and D. O'Neil, Phys. Rev. D **83**, 055017 (2011).

[31] R. Barbieri, L. J. Hall, and V. S. Rychkov, Phys. Rev. D **74,** 015007 (2006).

[32] G. Passarino and M. J. G. Veltman, Nucl. Phys. **B160**, 151 (1979).

[33] E. W. Kolb and M. S. Turner, *The Early Universe*, Frontiers in Physics (Westview Press, 1990), 1st ed., p. 596, https://doi.org/10.1201/9780429492860.

[34] P. Gondolo and G. Gelmini, Nucl. Phys. **B360**, 145 (1991).

[35] J. Edsjo and P. Gondolo, Phys. Rev. D **56**, 1879 (1997).

[36] H. Cai, T. Nomura, and H. Okada, Nucl. Phys. **B949**, 114802 (2019).